Rock and Soil Mechanics

Volume 41 | Issue 3 Article 1

9-27-2020

Upper bound analysis of the lateral bearing capacity of rigid piles in sloping ground

Ming-hua ZHAO

Wen-zhe PENG

Chao-wei YANG

Yao XIAO

See next page for additional authors

Custom Citation

ZHAO Ming-hua, PENG Wen-zhe, YANG Chao-wei, XIAO Yao, LIU Ya-nan. Upper bound analysis of the lateral bearing capacity of rigid piles in sloping ground[J]. Rock and Soil Mechanics, 2020, 41(3): 727-735.

Upper bound analysis of the lateral bearing capacity of rigid piles in sloping ground

Authors

Ming-hua ZHAO, Wen-zhe PENG, Chao-wei YANG, Yao XIAO, and Ya-nan LIU

Rock and Soil Mechanics 2020 41(3): 727−735 ISSN 1000−7598
https: //doi.org/10.16285/j.rsm.2019.5577 rocksoilmech.researchcommons.org/journal

Upper bound analysis of the lateral bearing capacity of rigid piles in sloping ground

ZHAO Ming-hua, PENG Wen-zhe, YANG Chao-wei, XIAO Yao, LIU Ya-nan
Institute of Geotechnical Engineering, Hunan University, Changsha, Hunan 410082, China

Abstract: This paper investigated the lateral ultimate bearing capacity of rigid pile in sloping ground. Firstly, the effective embedment depth of equivalent rigid piles of flexible piles and the mechanical characteristic of laterally loaded rigid piles are introduced. Secondly, two failure modes for the soil in front of laterally loaded piles are proposed under different directional loads at the top of piles (pointing toward and away from slope). Then, the ultimate bearing capacity of the rigid pile under different directional loads is derived on the basis of the upper limit theorem of limit-equilibrium analysis, and the rationality of the proposed method is verified by field tests. Finally, effects of the slope, internal friction angle, cohesion and load direction on the ultimate bearing capacity are investigated and some general conclusions are drawn. At the meantime, a fitting formula for the lateral ultimate bearing capacity of the rigid pile in sloping ground that considering the slope angle is proposed on the basis of the analysis results. References and guidance for design of piles in sloping ground are provided, which are valuable in both theoretical and engineering applications.

Keywords: bridge engineering; ultimate bearing capacity; limit-equilibrium analysis; laterally loaded rigid pile; sloping ground; failure mode

1 Introduction

Rigid piles are widely used in bridge piers, transmission towers and offshore platform foundations. During normal service, piles will inevitably bear the horizontal loads caused by vehicles, earthquakes and typhoons. In addition, in mountain highway bridge foundation, where buildings and transmission towers are built on sloping ground, the pile foundation has to be built in the slope ground due to the limitation of topography or highway alignment. At this time, the design of foundation pile should consider the influence of horizontal load and angle of slope. Because the deformation of rigid pile is usually negligible, most of the previous research focuses on the ultimate bearing capacity rather than the flexural deformation of foundation pile. It is worth mentioning that based on a large number of model tests of horizontally loaded piles, Meyerhof[1] and Sastry[2−4] put forward the concept of effective embedding depth of equivalent rigid piles of flexible piles, and extended some laws of rigid piles to flexible piles, which further enhanced the research value of horizontal ultimate bearing capacity of rigid piles.

At present, the researches on the lateral ultimate bearing capacity of rigid piles are mostly focused on rigid piles in flat ground. Meyerhof et al.[5−6] carried out horizontal static load tests on rigid piles in clay and sand to study the general law of the ultimate bearing capacity. Different from flexible pile[7], the research on rigid pile focused on ultimate bearing capacity. Since then, Cui et al.[8] discussed the instability mechanism of horizontally loaded rigid piles by carrying out horizontal loading tests of rigid piles in silty clay. Wang et al.[9] further analyzed the bearing mechanism of large diameter rock-socketed pile under horizontal load through the displacement of foundation pile and the resistance of foundation soil measured by field test. In recent years, Zhu et al.[10] studied the horizontal bearing characteristics of large diameter piles in sand through centrifugal model tests, and modified the initial stiffness of p–y curve based on the test results. In addition, numerical software[11−12] and theoretical model[13−17] are also gradually used to explore the horizontal bearing characteristics of rigid piles. It is worth noting that the upper limit theorem of limit equilibrium analysis is used to evaluate the horizontal bearing capacity of rigid piles in saturated clay and soil (c–φ) by Murff[13] and Cui[14], and its rationality is verified by experiments and numerical simulations. However, the above research objects are all on rigid piles in flat ground, and the calculation method of horizontal bearing capacity is not applicable to rigid piles in slope ground.

Some scholars have investigated the lateral ultimate bearing capacity of rigid piles in slope ground. Except for the simplified static equilibrium model put forward by Gabr and Borden[18], most of the other methods are based on numerical simulation[19−21] or experimental research[22−23]. Ng et al.[19]

Received: 26 March 2019 Revised: 27 May 2019
This work was supported by the National Natural Science Foundation of China(51478178).
First author: ZHAO Ming-hua, male, born in 1956, PhD, Professor, Doctoral supervisor, research interests: pile foundation and soft soil foundation treatment. E-mail: mhzhaohd@21cn.com

used three-dimensional numerical analysis method to study the load transfer mechanism of piles in slope foundation, and evaluated the influence of slope stability on the horizontal ultimate bearing capacity of rigid pile based on strength reduction method. Through three-dimensional finite element analysis, Georgiadis et al.[20−21] studied the bearing capacity of horizontally loaded rigid piles in slope foundation under undrained conditions, and deduced the horizontal ultimate bearing capacity of rigid piles in clay soil at a certain distance from the top of the slope by considering pile–soil interaction. Based on the prototype test and three-dimensional elastic-plastic finite element method, Chae et al.[22] analyzed the test results of single pile under horizontal load in a 30° slope of homogeneous sand. The influence of slope on horizontal bearing characteristics was discussed. Cheng et al.[23] adopted the method of model test and numerical simulation and proposed that the horizontal ultimate bearing capacity of rigid pile decreased with the increase of slope angle. The literature review shows that, compared with the foundation pile on the flat ground, the distribution form of earth pressure between piles in sloping ground under horizontal load is similar, and the soil resistance provided by the surrounding soil at the same depth is smaller. Compared with flat ground, the lateral ultimate bearing capacity of rigid piles in slope foundation decreased, which is related to slope and soil strength index. However, most of the above studies are based on experiments or numerical simulations, therefore, it is inconvenient to be used in the preliminary design. In addition, the influence of the slope on the ultimate failure mode of the rigid pile and the working condition of the pile top load pointing to the slope at the arch foot of the arch bridge in the mountain area were not considered in the previous literatures.

Based on the literature, this paper aimed to investigate the slope foundation and rigid pile from the following aspects: (i)The concept of effective embedding depth of equivalent rigid pile and the reaction distribution model of limit horizontal foundation is briefly introduced; (ii)Two cases that the load points to the outside of the slope and inside the slope are considered, two ultimate failure modes suitable for the soil in front of the rigid pile in the slope foundation are put forward, respectively; (iii)Based on the upper limit theorem of limit equilibrium analysis, the ultimate bearing capacity of rigid piles under two load directions is derived, and the upper limit solution of limit equilibrium analysis is verified by field tests; (iv)The effects of slope angle, internal friction angle, cohesion and load direction on the ultimate bearing capacity are discussed in order to improve the theoretical study of slope foundation pile design.

2 Effective embedding depth and ultimate horizontal reaction force

2.1 The effective embedding depth of equivalent rigid pile

As shown in fig. 1, Meyerhof[1] and Sastry[2−4] thought that flexible piles were equivalent to rigid piles in a certain depth, and the method for determining the equivalent pile length was detailed in references[1−4]. Based on the research work of Meyerhof et al.[1], the rigid piles are fully studied and then extended to the general situations (flexible piles or semi-flexible piles), which can provide some reference for the study of horizontal bearing capacity of flexible piles in the future. Since research object of this paper is the rigid pile, the equivalent process will not be described in detail. In the figure: h is the length of flexible pile; h_e is the equivalent rigid pile length under horizontal load H; h_{eu} and δ_u are the equivalent rigid pile length and equivalent rotation angle when the horizontal load reaches its ultimate bearing capacity H_u, respectively.

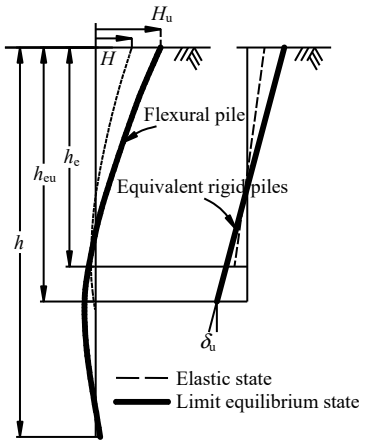

Fig.1 The effective embedment depth of equivalent rigid piles

2.2 Distribution of ultimate reaction force (soil resistance) of pile foundation in flat ground

Guo[15] and Qin[16] believed that with the increase of horizontal load H and horizontal displacement u_0 at the top of pile, the distribution of reaction force of pile foundation may appear in three stages as shown in Fig.2: (a)Pile top yield stage (see Fig.2(a)), z_r is the depth of the center of rotation, and the reaction force of the foundation reaches the limit state in the depth of 0–z_0. (b) Pile bottom yield stage (see Fig.2(b)), the rotation angle continues to increase, z_0 continues to deepen, and the foundation reaction below the z_1 depth begins to enter the limit equilibrium state. (c) Ultimate yield stage (see Fig.2(c)), with the continuous increase of the load, the reaction of the whole foundation reaches the limit equilibrium state. p_u and u^* are the ultimate soil resistance and its corresponding soil

displacement varying with depth, which satisfies the load transfer model shown in Fig.3[15−16]. u is the displacement of the foundation pile; p is the soil resistance.

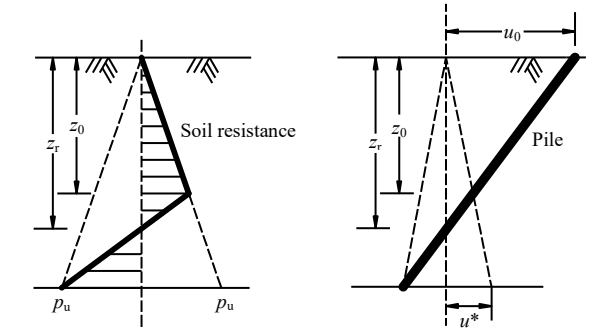

(a) Pile top yield stage

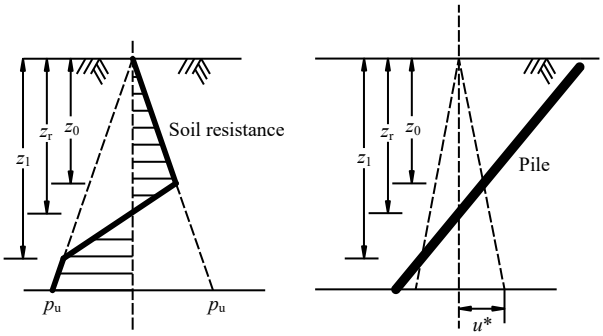

(b) Pile bottom yield stage

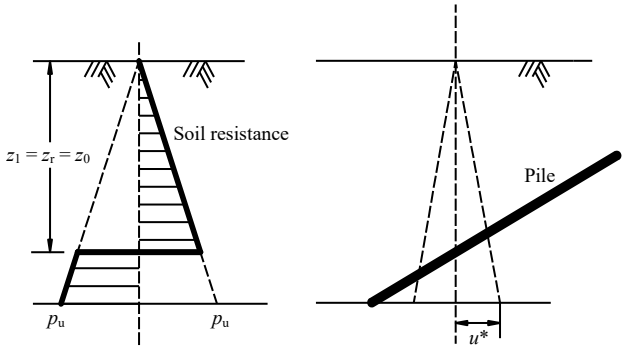

(c) Ultimate yield stage

Fig.2 Profiles of the ultimate soil resistance, surrounding soil resistance and pile deformation

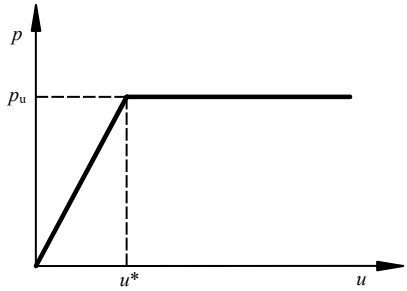

Fig.3 Load transfer model

3 Basic assumptions and soil ultimate failure mode

In engineering practice, especially in the slope ground, the pile foundation of the bridge usually bears very complex loads from the superstructures, including wind load, vehicle braking force and other horizontal loads in addition to the vertical load. In particular, when the bridge is an arch bridge and crosses the gully, the pile foundation at the foot of the arch is subjected to a horizontal load pointing to the inside of the slope[24−25], as shown in Fig.4.

Fig.4 Daxiaojing super bridge

When the rigid pile in the slope foundation bears horizontal load, ultimate failure surfaces in the slope may appear as shown in Fig.5. Based on the upper bound theorem of limit equilibrium analysis, this paper makes the following assumptions:

(1) When the horizontal load points to the outside direction of the slope, the slope will be destroyed along BO or BO', and two types of failure surfaces may appear as shown in Fig.6 (the angle ABO is less than 90^0 and the angle ABO' is more than 90^0). When the horizontal load points to the slope, the slope will be destroyed along $BCDE$(see Fig.5), in which $BCDE$ is composed of straight line BC, logarithmic spiral CD and straight line DE. In the figure: L is the length of the rigid pile; L_r is the distance from the top of the pile to the center of rotation; p_{u1} is the ultimate soil resistance at the center of rotation; p_{u2} is the ultimate soil resistance at the bottom of the pile; and μ' is the angle between the failure surface $B'O'$ and the slope surface.

(2) The wedge ABC and ADE are isosceles triangles. The angle μ between the failure surface and the slope and the internal friction angle φ satisfies this formula: $\mu = 45°–\varphi/2$, the angle α corresponding to the logarithmic helix is equal to the slope angle θ.

(3) When the horizontal load reaches its ultimate bearing capacity, the soil reaction force distribution of the foundation is shown in Figs. 6 and 7.

4 Upper bound limit equilibrium analysis of lateral bearing capacity of rigid piles in slope foundation

The basic idea of the upper bound limit equilibrium analysis

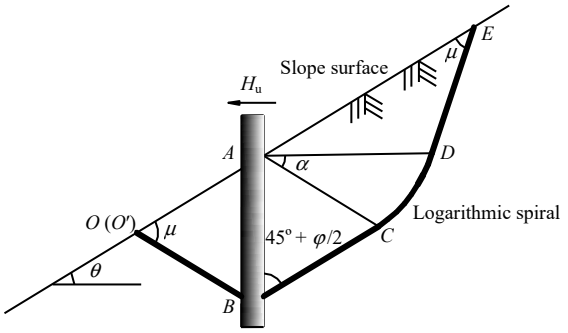

Fig.5 Failure modes of soils in front of rigid piles in sloping ground

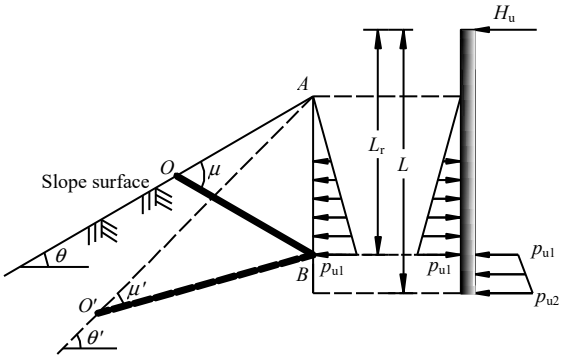

Fig.6 Foundation soil reaction under lateral ultimate loads pointing away from slope

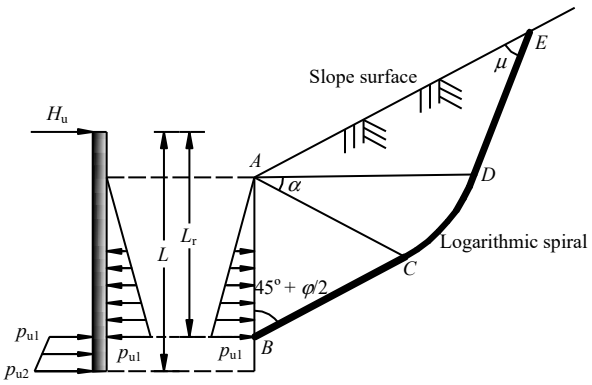

Fig.7 Foundation soil reaction under lateral ultimate loads pointing toward slope

is that for the assumed limit failure mode, when the external force, including dead weight, exceeds its internal resistance (energy dissipation), the slope will be destroyed. Based on the principle of virtual work, the virtual power equation can be established:

$$\sum E = \sum W + \sum P \tag{1}$$

where $\sum E$ is the energy loss rate; $\sum W$ is the self-weight work power of soil; $\sum P$ is the work power under external load.

4.1 The lateral load points outside of the slope

When the load points in the direction outside of the slope, the soil in front of the pile can be regarded as an acute angle wedge. Chen[26] thought that the simplest form of the acute angle wedge failure mechanism can be represented by plane sliding, as shown in Fig.8. Below the failure line *BO* or *BO′* (broken line), the soil remains static. According to the properties of Coulomb materials in accordance with the associated flow rule, the relative velocity of each point on the broken line is at an angle φ to the direction of the shear force.

When the slope angle θ and the internal friction angle φ satisfy the following formula, the slope is destroyed along the *BO*:

$$45° + \varphi/2 + \theta > 90° \tag{2}$$

When the slope angle θ and the internal friction angle φ change to θ' and φ', which satisfies the following formula, the slope is destroyed along the *BO′* (in the following formula derivation, θ, φ and μ can be replaced by the corresponding θ', φ' and μ').

$$45° + \varphi'/2 + \theta' < 90° \tag{3}$$

The internal energy dissipation rate on the *BO* line is

$$D_{BO} = cl_{BO}V\cos\varphi = cl_{AB}V\frac{\cos\varphi\cos\theta}{\sin\mu} \tag{4}$$

where l_{BO} and l_{AB} are the length of lines *BO* and *AB*, respectively; and *V* is the velocity field of wedges *ABO* or *ABO′*. The self-weight work W_{ABO} of wedge-shaped *ABO* is

$$W_{ABO} = \frac{1}{2}\gamma l_{AB}^2 V\frac{\cos\theta\cos(\mu-\theta)\sin(\theta-\mu-\varphi)}{\sin\mu} \tag{5}$$

where γ is the unit weight of the soil.

The work power of external load *P* is

$$P = \frac{1}{2}p_{u1}l_{AB}V\cos(\mu+\varphi-\theta) \tag{6}$$

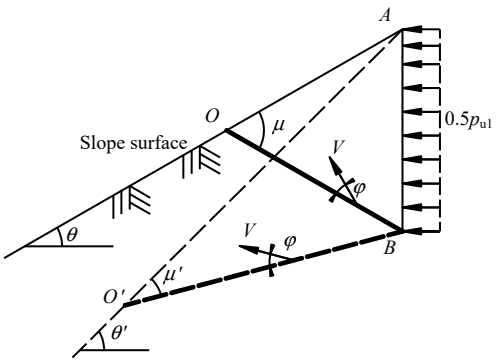

Fig.8 Velocity field of slope when lateral ultimate loads point away from slope

4.2 The lateral load points into the slope

When the load points in the slope, the soil in front of the

pile can be regarded as an obtuse wedge. Chen[26] thought that the failure mechanism of the obtuse wedge is composed of triangular areas *ABC* and *ADE* moving as a rigid body and a logarithmic spiral zone *ACD*, as shown in Fig.9. Below the failure line *BCDE* (velocity broken line), the soil remains static. In the logarithmic spiral region *ACD*, the velocity increases exponentially from the initial velocity V_0 of the radiation *AC* to the velocity *V* of the radiation *AD*.

$$V = V_0 \mathrm{e}^{\alpha \tan \varphi} \tag{7}$$

where α is the angle between line *AC* and line *AD* in Figs. 5 and 7.

The energy loss rate D_{ACD} of *ACD* in logarithmic helix region is equal to that of D_{CD} on logarithmic helix *CD*, and its value is

$$D_{CD} = D_{ACD} = \frac{1}{2} c V_0 l_{AC} \cot \varphi \left(\mathrm{e}^{2\alpha \tan \varphi} - 1 \right) \tag{8}$$

Rigid body *ABC* and *ADE* have internal energy dissipation on *BC* and *DE*, respectively, and their loss rates D_{BC} and D_{DE} are

$$D_{BC} = c l_{BC} V_0 \cos \varphi = c l_{AB} V_0 \sin(\mu + \varphi) \tag{9}$$

$$D_{DE} = c l_{DE} V \cos \varphi = c l_{AB} V_0 \mathrm{e}^{2\alpha \tan \varphi} \sin(\mu + \varphi) \tag{10}$$

The self-weight work power W_{ACD} of *ACD* in logarithmic spiral region is

$$W_{ACD} = \frac{1}{2} \gamma \int_0^{\alpha} l_{AB}^2 V_0 \frac{\sin^4(\mu + \varphi) \cos(\delta + \varphi)}{\cos^2 \varphi} \mathrm{d}\delta \sec \varphi \mathrm{e}^{3\alpha \tan \varphi} \tag{11}$$

The self-weight work W_{ABC} and W_{ADE} of rigid body *ABC* and *ADE* are

$$W_{ABC} = \frac{1}{2} \gamma l_{AB}^2 V_0 \frac{-\sin^3(\mu + \varphi)}{\cos \varphi} \tag{12}$$

$$W_{ADE} = \frac{1}{2} \gamma l_{AB}^2 V_0 \mathrm{e}^{3\alpha \tan \varphi} \sin^4(\mu + \varphi) \tag{13}$$

The working power of external load is

$$P = \frac{1}{2} p_{\mathrm{u}1} l_{AB} V \cos(\mu + \varphi) \tag{14}$$

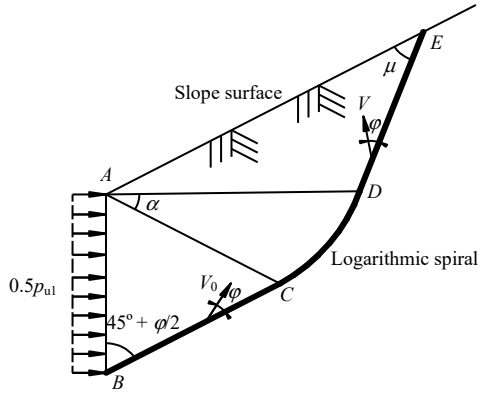

Fig.9 Velocity field of slope when lateral ultimate loads point toward slope

4.3 Derivation process of lateral ultimate bearing capacity

Based on the above analysis, the calculation process of lateral ultimate bearing capacity of rigid piles in slope foundation is as follows:

(1) Assuming the position of the center of rotation (similar to assume the length of the L_r), and substituting the Eqs.(4)–(6) or the Eqs.(7)–(14) into the Eqs.(1), when the load points to the outside or inside the slope, the p_{u1} can be obtained.

(2) The p_{u2} can be obtained by taking the moment at the action point of the horizontal load (that is, the top of the pile).

(3) Compare p_{u2} and p_u. If $p_{u2}<p_u$, increase L_r and repeat the process (2) and process (3); if $p_{u2}>p_u$, decrease L_r and repeat process (2) and process (3); if $p_{u2}=p_u$, enter process (4).

(4) Based on the static equilibrium analysis of rigid piles, the horizontal ultimate bearing capacity H_u of rigid piles on slope foundation can be obtained.

It is worth noting that in engineering practice, the ultimate soil resistance of rigid piles does not necessarily have the triangular distribution shown in Figs. 6 and 7. Zhang[17] believed that the horizontal foundation reaction distribution of rigid pile under the limit state may be in the form of rectangle, triangle, trapezoid, etc. Georgiadis et al.[21] believed that the distribution of the ultimate horizontal foundation reaction in front of rigid pile on slope foundation may be in the form of nonlinear distribution with increase of depth.

Therefore, it is necessary to select the appropriate distribution form according to the slope soil properties and engineering practice. If the condition is limited, it can be calculated according to each form, and the minimum value of H_u is selected as its ultimate bearing capacity, which is safe in engineering design.

5 Case study

In order to verify the rationality of the theoretical method developed in this paper, the examples in reference [21] and reference [17] are introduced for comparative analysis. To simplify the calculation process, the soil reaction distribution of lateral bearing capacity is assumed to be triangular distribution. Georgiadis et al.[21] compared its theoretical analysis results with the field test results of horizontally loaded rigid pile on slope foundation of Bhushan et al.[27]. The pile test is shown as follows: pile length L = 5.18 m, pile diameter D = 1.22 m, distance of horizontal load from ground e = 0.23 m, slope angle θ = 20°, soil is saturated clay, cohesion c_u = 220 kPa. The theoretical results (1) and (2) are the calculated values with and without considering the cohesion of pile–soil interface.

As can be seen from Table 1:

(1) The theoretical values from this paper are close to the experimental and theoretical values in the literatures, which

shows that the theoretical value obtained by the upper bound method of limit equilibrium analysis in this paper is feasible to predict the horizontal ultimate bearing capacity of rigid piles in the slope ground (the load points off the slope).

(2) Compared with the theoretical value in reference[21], the theoretical value from this paper is closer to the experimental value. The main reason is that in the theoretical calculation, Georgiadis et al.[21] reduced the ultimate reaction force, and failed to consider the influence of the horizontally loaded pile on the slope stability, thus the calculation result may be too large.

Table 1 Comparisons of measured results and analytical results of horizontal ultimate bearing capacity

Results type	Theoretical value /kN	Test value[27] /kN	Error/%
Theoretical value 1[21]	2 835	2 180	+30.0
Theoretical value 2[21]	2 518	2 180	+15.5
This paper	2 102	2 180	−3.6

(3) The theoretical value of this paper is the minimum, which shows that the ultimate bearing capacity obtained by the method in this paper is on the safe side.

Zhang et al.[17] compared their theoretical analysis results with the lateral load field test results on rigid piles in flat ground (regarded as a special case of $a = 0$ when the load points to the slope) of Helmers[28] and Choi[29].

The basic parameters of pile test from Helmers et al.[28] is shown as follows: the length of the pile is 2.44 m, the diameter of the pile is 0.2 m, the distance between the horizontal load and the ground is 1.22 m, and the other conditions are shown in Table 2.

The basic parameters of pile tests of Choi et al.[29] are shown as follows: pile diameter D = 0.4 m, weight of soil γ = 18 kN/m^3, cohesion c = 20 kPa, internal friction angle φ = 30°, and other conditions are shown in Table 3.

As can be seen from tables 2 and 3:

(1) The theoretical value of this paper is similar to the

Table 2 Comparisons of measured results (Helmers et al[28]) and analytical results of horizontal ultimate bearing capacity

γ/(kN • m^{-3})	c/kPa	φ/(°)	Test value[28]/kN				Average value[28] /kN	Theoretical value[17] /kN	Error[17] /%	Theoretical value by this paper/kN	Error/%
			Test 1	Test 2	Test 3	Test 4					
19.1	17.3	31	14.3	19.5	21.6	19.4	18.7	17.5	−6.4	19.3	+3.2
16.8	20.0	34	27.7	27.1	27.1	24.4	26.6	23.7	−10.9	22.7	−14.7
16.8	19.2	31	27.7	25.8	25.6	24.4	25.9	17.9	−30.9	21.0	−18.9

Note: The error in table 2 is the error between the theoretical value and the experimental value[28].

Table 3 Comparisons of measured results (Choi et al.[29]) and analytical results

No.	L/m	e/m	Test value[29] /kN	Theoretical value[17] /kN	Error[17] /%	Theoretical value by this paper /kN	Error /%
1	3.20	2.00	26	24	−7.7	33	+26.9
2	4.40	2.00	52	115	+121.1	108	+107.7
3	2.55	0.15	211	212	+0.5	209	−0.9

Note: The error in table 3 is the error between the theoretical value and the experimental value[29].

experimental and theoretical value of the literature, and the error with the test is mostly less than 30%. It shows that the theoretical value obtained by the upper limit method of limit analysis in this paper is feasible to predict the horizontal ultimate bearing capacity of rigid piles on the slope foundation (the load points to the slope).

(2) Compared with the tests 1 and 2 of Choi et al.[29], the theoretical calculation method used to predict test 3 is closer to the test value, indicating that the upper bound method of limit equilibrium analysis is more reasonable to predict the ultimate bearing capacity when the load is close to the ground.

6 Influence of slope and load direction

In order to discuss the influence of slope and load direction on the lateral ultimate bearing capacity of rigid pile, it is assumed that a rigid pile is located in the slope. The parameters of slope and rigid pile are shown in Table 4, where E_s is the elastic modulus of soil and ν_s is Poisson's ratio of soil. Taking this condition as the basis, the ultimate bearing capacity based on the theoretical method is solved by changing the slope, internal friction angle, cohesion and load direction, which is drawn in Figs. 10–12.

Figure 10 shows the variation of ultimate bearing capacity with the change of slope and load direction. In the figure, the slope θ of "+" indicates that the load is pointing inside the slope, and θ of "–" indicates that the load is pointing outside the slope. It can be seen from the diagram that when the load points to the inside of the slope, the greater the slope, the greater the ultimate

bearing capacity; when the load points to the outside direction of the slope, the greater the slope, the smaller the ultimate bearing capacity.

Figures 11 and 12 show the effects of internal friction angle and cohesion on the ultimate bearing capacity, respectively. As can be seen from the picture:

Table 4 Basic parameters of pile and soil

Structure type	γ/(kN • m^{-3})	E_s/MPa	v_s	φ/(°)	c/kPa
Pile	24	30 000	0.2	—	—
Slope	20	50	0.3	30	25

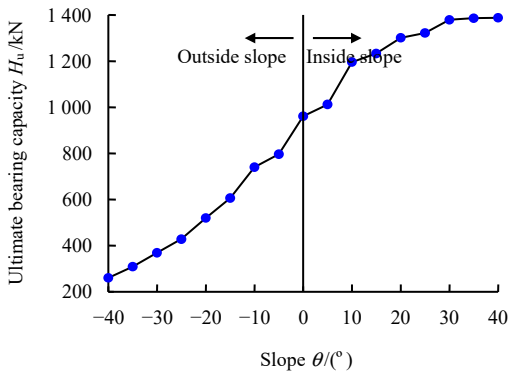

Fig.10 Effects of slope and load direction on ultimate bearing capacity

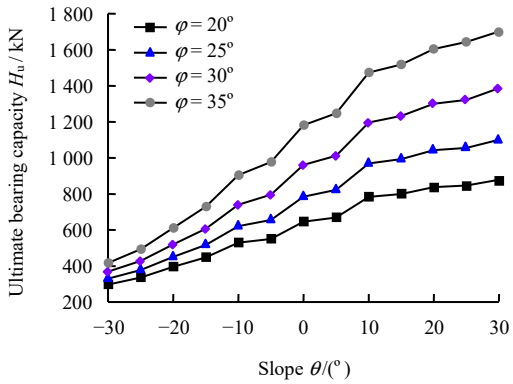

Fig.11 Effect of internal friction angle on ultimate bearing capacity

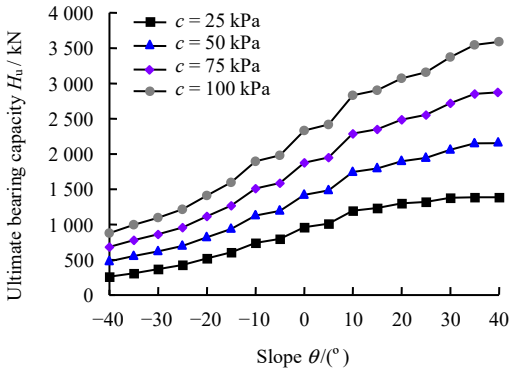

Fig.12 Effect of cohesion on ultimate bearing capacity

(1) With the increase of the angle of internal friction and cohesion, the ultimate bearing capacity increases, indicating that the improvement of soil strength is helpful to improve the lateral ultimate bearing capacity.

(2) The slope of ultimate bearing capacity with the change of slope angle increases with the increase of internal friction angle and cohesion, indicating that the higher the strength of soil is, the more obvious the influence of slope on ultimate bearing capacity is.

In order to further explore the influence of slope and load direction on ultimate bearing capacity, the slope influence coefficient η and load direction influence coefficient χ are put forward. Among them, the influence coefficient of the slope is defined as the ratio of the ultimate bearing capacity in the slope to the ultimate bearing capacity in the flat ground, and the influence coefficient of the load direction is the ratio of the ultimate bearing capacity of the horizontal load pointing to the inside and outside the slope at the same grade of slope.

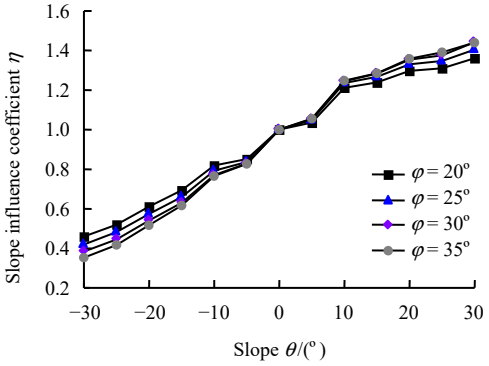

Fig.13 Effect of internal friction angle on influence coefficient of slope

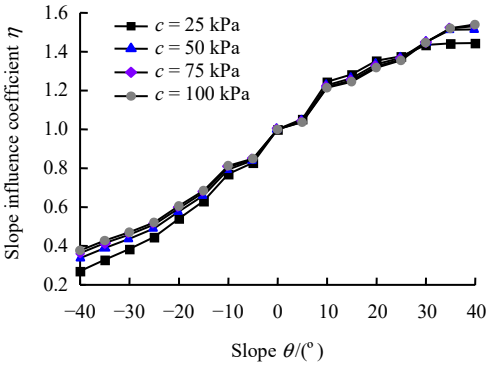

Fig.14 Effect of the cohesion on the influence coefficient of slope

Figures 13 and 14 show the influence of internal friction angle and cohesion on the slope influence coefficient, respectively. It can be seen from the diagram that under different internal friction angles and cohesions, the increase/decrease trend of slope to ultimate bearing capacity is

basically the same, and each curve is in good agreement with each other. Therefore, this paper will use cubic polynomials to fit the 8 curves in Figs. 13 and 14 so as to establish relationships of bearing capacity of rigid piles between in the sloping foundation and in flat ground. As shown in Eq. (15), the regression equation has the coefficient $R^2 = 0.99$.

$$\eta = -6\times10^{-6}\theta^3 - 9\times10^{-5}\theta^2 + 0.0218\theta + 0.9822$$

$$(-40° \leqslant \theta \leqslant 40°) \tag{15}$$

Figures 15 and 16 show the influence of internal friction angle and cohesion on the load direction, respectively. It can be seen from the picture:

(1) With the increase of the slope angle, the influence of the load direction on the ultimate bearing capacity is more obvious, because when the slope angle increases, the load points to the slope, which leads to more soil failure as the load increases, and more resistance from the slope weight and friction can be provided; when the load points to the outside of the slope, it reduces the chances of soil failure, and the resistance decreases accordingly.

(2) The load direction influence coefficient is positively correlated with the internal friction angle, indicating that the increase of the bearing capacity with increasing the internal friction angle when the load is directed into the slope is higher than that when the load is directed the outside of the slope.

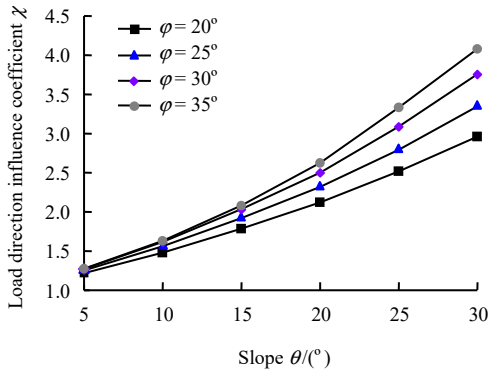

Fig.15 Effect of the internal friction angle on the influence coefficient of load direction

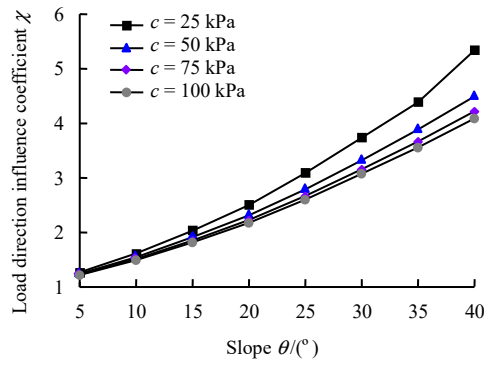

Fig.16 Effect of the cohesion on the influence coefficient of load direction

(3) The influence coefficient of load direction is negatively correlated with cohesive force, indicating that the increase of the bearing capacity with increasing the cohesive force when the load is pointing into the slope is lower than that when the load is pointing the outside of the slope.

7 Conclusions

(1) In view of the two cases where the horizontal load points the outside of the slope and inside of the slope, two ultimate failure modes that suitable for the soil in front of the rigid piles of the slope foundation were proposed.

(2) Based on the upper bound theorem of limit equilibrium analysis, the ultimate bearing capacity of the rigid pile under two load directions was derived; and the feasibility of the theoretical method in this paper was verified by field tests.

(3) The effects of slope angle, internal friction angle, cohesion and load direction on the ultimate bearing capacity were discussed, and some general conclusions were drawn. Slope influence coefficient η and load direction influence coefficient χ were proposed. The formula of η changing with slope angle was fitted by cubic polynomial, which was used to establish the relationship between the bearing capacity of rigid pile on slope foundation and flat ground. The general laws of χ with internal friction angle and cohesion were discussed.

References

[1] MEYERHOF G G, GHOSH D P. Ultimate capacity of flexible piles under eccentric and inclined loads[J]. Canadian Geotechnical Journal, 1989, 26(1): 34–42.

[2] SASTRY V, MEYERHOF G G. Behaviour of flexible piles under inclined loads[J]. Canadian Geotechnical Journal, 1990, 27(1): 19–28.

[3] SASTRY V, MEYERHOF G G. Behaviour of flexible piles in layered sands under eccentric and inclined loads[J]. Canadian Geotechnical Journal, 1994, 31(4): 513–520.

[4] SASTRY V, MEYERHOF G G. Behaviour of flexible piles in layered clays under eccentric and inclined loads[J]. Canadian Geotechnical Journal, 1995, 32(3): 387–396.

[5] MEYERHOF G G. The bearing capacity of rigid piles and pile groups under inclined loads in clay[J]. Canadian Geotechnical Journal, 1981, 18(2): 297–300.

[6] MEYERHOF G G, MATHUR S K, VALSANGKAR A J. The bearing capacity of rigid piles and pile groups under inclined loads in layered sand[J]. Canadian Geotechnical

Journal, 1981, 18(4): 514–519.

[7] ZHU Ming-xing, DAI Guo-liang, GONG Wei-ming, et al. Mechanism and calculation models of resisting moment caused by shaft resistance for laterally loaded pile[J]. Rock and Soil Mechanics, 2019, 40(7): 2593–2607, 2662.

[8] CUI Xin-zhuang, DING Hua. Experimental study on instability of rigid piles under lateral loads in silty clay[J]. Rock and Soil Mechanics, 2004, 25(11): 1744–1748, 1753.

[9] WANG Jian-hua, CHEN Jin-jian, KE Xue. Characteristics of large diameter rock-socketed piles under lateral loads[J]. Chinese Journal of Geotechnical Engineering, 2007, 29(8): 1194–1198.

[10] ZHU Bin, XIONG Gen, LIU Jin-chao, et al. Certrifuge modeling of a large-diameter single pile under lateral loads in sand[J]. Chinese Journal of Geotechnical Engineering, 2013, 35(10): 1807–1815.

[11] LIU Jin-chao, XIONG Gen, ZHU Bin, et al. Bearing capacity and deflection behaviors of large diameter monopile foundations in sand seabed[J]. Rock and Soil Mechanics, 2015, 36(2): 591–599.

[12] WANG Jun-lin, WANG Fu-ming, REN Lian-wei, et al. Horizontal static load test and numerical simulation of single large diameter under-reamed pile[J]. Chinese Journal of Geotechnical Engineering, 2010, 32(9): 1406–1411.

[13] MURFF J D, HAMILTON J M. *P*-ultimate for undrained analysis of laterally loaded piles[J]. Journal of Geotechnical Engineering, 1993, 119(1): 91-107.

[14] CUI Xin-zhuang, DING Hua, JIN Qing, et al. Three-dimensional limit analysis of lateral bearing capacity of rigid piles[J]. Chinese Journal of Rock Mechanics and Engineering, 2006, 25(3): 641–646.

[15] GUO W D. Laterally loaded rigid piles in cohesionless soil[J]. Canadian Geotechnical Journal, 2008, 45(45): 676–697.

[16] QIN H Y, GUO W D. Limiting force profile and laterally loaded rigid piles in sand[C]//Applied Mechanics and Materials. [S. l.]: Trans. Tech. Publications, 2014: 452–457.

[17] ZHANG W M. Ultimate lateral capacity of rigid pile in *c*-*φ* soil[J]. China Ocean Engineering, 2018, 32(1): 41–50.

[18] GABR M A, BORDEN R H. Lateral analysis of piers constructed on slopes[J]. Journal of Geotechnical Engineering, 1990, 116(12): 1831–1850.

[19] NG C W, ZHANG L M, HO K K. Influence of laterally loaded sleeved piles and pile groups on slopes[J]. Canadian Geotechnical Journal, 2001, 38(3): 553–566.

[20] GEORGIADIS K, GEORGIADIS M. Undrained lateral pile response in sloping ground[J]. Journal of Geotechnical and Geoenvironmental Engineering, 2010, 136(11): 1489–1500.

[21] GEORGIADIS K, GEORGIADIS M, ANAGNOSTOPOULOS C. Lateral bearing capacity of rigid piles near clay slopes[J]. Soils and Foundations, 2013, 53(1): 144–154.

[22] CHAE K S, UGAI K, WAKAI A. Lateral resistance of short single piles and pile groups located near slopes[J]. International Journal of Geomechanics, 2004, 4(2): 93–103.

[23] CHENG Liu-yong, XU Xi-chang, CHEN Shan-xiong, et al. Model test and numerical simulation of horizontal bearing capacity and impact factors for foundation piles in slope[J]. Rock and Soil Mechanics, 2014, 35(9): 2685–2691.

[24] ZHANG Xiang-bing. Rainbows on the Daxiaojing- the new member of the ‘World Bridge Museum’[J]. China Highway, 2018, 25(14): 78–79.

[25] WANG Ya-wei. Construction techniques for erection of arch rib of main bridge of Guizhou Yachi River Bridge on Chengdu-Guiyang Railway[J]. Bridge Construction, 2017, 47(1): 104–108.

[26] CHEN Hui-fa. Limit analysis and soil plasticity[M]. Beijing: China Communications Press, 1995.

[27] BHUSHAN K, HALEY S C, FONG P T. Lateral load tests on drilled piles in stiff clays[J]. Journal of the Geotechnical Engineering Division, 1979, 105(8): 969–985.

[28] HELMERS M J, DUNCAN J M. Ultimate load design of laterally loaded drilled shaft foundations[M]//New Technological and Design Developments in Deep Foundations. 2000: 207–223.

[29] CHOI H Y, LEE S R, PARK H I, et al. Evaluation of lateral load capacity of bored piles in weathered granite Soil[J]. Journal of Geotechnical and Geoenvironmental Engineering, 2013, 139(9): 1477–1489.